REVIEW ARTICLE

*CONTINUUM* AUDIO INTERVIEW AVAILABLE ONLINE

# The Value of Neuroimaging in Dementia Diagnosis

By Cyrus A. Raji, MD, PhD; Tammie L. S. Benzinger, MD, PhD

**CITE AS:**
CONTINUUM (MINNEAP MINN) 2022;28(3, DEMENTIA):800–821.

Address correspondence to Dr Cyrus A. Raji, Neuromagnetic Resonance Imaging, Washington University School of Medicine, Mallinckrodt Institute of Radiology, 4525 Scott Ave, Campus Box 8131, St. Louis, MO 63110, craji@wustl.edu.

**RELATIONSHIP DISCLOSURE:**
Dr Raji has received personal compensation in the range of $10,000 to $49,999 for serving as a consultant for Brainreader A/S, on a scientific advisory or data safety monitoring board for Apollo Health, and as an expert witness for Neurevolution Medicine, LLC. The blood-based amyloid test is licensed by C2N and was cofounded by colleagues of Dr Raji. Washington University will receive royalties from this test, but Dr Raji will not receive personal compensation from it. Dr Benzinger has received personal compensation in the range of $5000 to $9999 for serving as a consultant, on a scientific advisory or data safety monitoring board, and on a speakers bureau for Biogen. Dr Benzinger has noncompensated relationships
*Continued on page 821*

**UNLABELED USE OF PRODUCTS/INVESTIGATIONAL USE DISCLOSURE:**
Drs Raji and Benzinger discuss unlabeled/investigational uses of amyloid and tau positron emission tomography for the diagnosis of dementia.



## ABSTRACT

**PURPOSE OF REVIEW: This article discusses neuroimaging in dementia diagnosis, with a focus on new applications of MRI and positron emission tomography (PET).**

**RECENT FINDINGS: Although the historical use of MRI in dementia diagnosis has been supportive to exclude structural etiologies, recent innovations allow for quantification of atrophy patterns that improve sensitivity for supporting the diagnosis of dementia causes. Neuronuclear approaches allow for localization of specific amyloid and tau neuropathology on PET and are available for clinical use, in addition to dopamine transporter scans in dementia with Lewy bodies and metabolic studies with fludeoxyglucose PET (FDG-PET).**

**SUMMARY: Using computerized software programs for MRI analysis and cross-sectional and longitudinal evaluations of hippocampal, ventricular, and lobar volumes improves sensitivity in support of the diagnosis of Alzheimer disease and frontotemporal dementia. MRI protocol requirements for such quantification are three-dimensional T1-weighted volumetric imaging protocols, which may need to be specifically requested. Fluid-attenuated inversion recovery (FLAIR) and 3.0T susceptibility-weighted imaging (SWI) sequences are useful for the detection of white matter hyperintensities as well as microhemorrhages in vascular dementia and cerebral amyloid angiopathy. PET studies for amyloid and/or tau pathology can add additional specificity to the diagnosis but currently remain largely inaccessible outside of research settings because of prohibitive cost constraints in most of the world. Dopamine transporter PET scans can help identify Lewy body dementia and are thus of potential clinical value.**

## INTRODUCTION

Neuroimaging traditionally has played a focused role in the diagnosis of dementia. For Alzheimer disease (AD), the most common cause of dementia worldwide,[1] neuroimaging has historically been used to rule out structural causes of dementia,[2] including large strokes, brain tumors, infectious causes, and, in rare cases, reversible vascular causes such as dural arteriovenous fistulas.[3-5] When using neuroimaging

in dementia, several points should be emphasized. First, MRI is a widely available modality, with a total 40 million MRI scans done in the United States in 2019[6,7] across almost 12,000 MRI scanners and all bodily organs compared to a total 2 million positron emission tomography (PET) scans[8] for all indications across about 2500 PET scanners. Also, the cost of an MRI is much less than the cost of a PET scan; in the United States, a noncontrast brain MRI costs as little as $437 compared to about $2700 for a brain fludeoxyglucose PET (FDG-PET) scan.[9] For perspective, the cost of an MRI in the Netherlands is $190,[10] further highlighting the relatively low cost of MRI internationally. Also, brain MRI is the first-line neuroimaging modality recommended in the imaging guidelines for dementia as published by the American Academy of Neurology,[2] National Institute on Aging,[11] and American College of Radiology[12]; CT also can be recommended, especially when MRI cannot be accomplished (eg, when a patient has a pacemaker). These recommendations are mirrored in the American College of Radiology Appropriateness Criteria, which recommend CT of the head or MRI without contrast. However, because head CT has lower anatomic resolution than MRI, particularly for regional quantification,[13] it is reduced in sensitivity for detecting atrophy in neurodegenerative disease and is exceeded by MRI for detecting vascular disease.[14] Based on a combination of patient access, financial costs, anatomic resolution, and formal society guidelines, brain MRI is the main focus of this article, with additional commentary on the role of FDG-PET in complex cases and of amyloid and tau PET in clinical trials and emerging therapeutic strategies for AD and related dementias.

## MRI PROTOCOL CONSIDERATIONS

The minimum elements of a dedicated dementia MRI protocol should include a high-resolution T1-weighted imaging sequence to allow for quantitative analysis of specific brain atrophy patterns. To evaluate for vascular pathology, the protocol should also include diffusion-weighted MRI sequences to detect acute infarction, as ongoing infarcts may present as sudden memory loss.[15] T2-weighted and fluid-attenuated inversion recovery (FLAIR) sequences allow for assessment of white matter disease, whereas blood-sensitive susceptibility-weighted sequences enable evaluation for cerebral microhemorrhages.[16] These microhemorrhages are caused by structural abnormalities of small cerebral blood vessels that generally relate to cerebral amyloid angiopathy (CAA) or to hypertensive vasculopathy in dementia populations. Additional sequences may also be helpful for clinical evaluation or research but may be difficult to use in older individuals as longer scan times may not be tolerated, leading to increased motion or premature cessation of the imaging study. For volumetric acquisitions, the three-dimensional T1-weighted scan is used; this scan has different designations but is most commonly called either a magnetization prepared rapid gradient echo (MPRAGE) sequence or a spoiled gradient recalled acquisition (SPGR) sequence, depending on manufacturer. Standardized protocols are available for download from the Alzheimer's Disease Neuroimaging Initiative (adni.loni.usc.edu/methods/documents/mri-protocols) and National Institute on Aging (scan.naccdata.org).

Use of gadolinium contrast is not recommended for dementia evaluation unless clinical suspicion exists of a neoplastic, infectious, or inflammatory process. The most common field strengths of scanners are 1.5T and 3.0T, with lower field strengths occasionally encountered on open MRI machines. In

### KEY POINTS

- Brain MRI is the first-line neuroimaging as recommended by the American Academy of Neurology, National Institute on Aging, and American College of Radiology imaging guidelines for dementia, although CT is also recommended as an alternative.
- The minimum elements of a dedicated dementia MRI protocol should include a high-resolution T1-weighted imaging sequence to allow for quantitative analysis of specific brain atrophy patterns.
- For volumetric acquisitions, the three-dimensional T1-weighted scan is used; this scan has different designations but is most commonly called either a magnetization prepared rapid gradient echo (MPRAGE) sequence or a spoiled gradient recalled acquisition (SPGR) sequence, depending on manufacturer.

general, patients should be scanned on either 1.5T or 3.0T machines as either field strength can detect brain atrophy related to neurodegenerative disease.[17] However, 3.0T scanners are preferred, when available, as they allow for the acquisition of sequences such as susceptibility-weighted imaging (SWI) that optimize evaluation of hemorrhage. When considering longitudinal analysis in patients to track brain volume changes, it is important to image on scanners that have the same field strength and vendor.

## POTENTIAL PITFALLS

When considering neuroimaging for cognitive decline, several caveats should be considered. Appropriate imaging should include correct sequences as detailed previously, such as three-dimensional T1-weighted sequences for volumetric quantification as well as susceptibility-sensitive sequences to detect microhemorrhages, particularly for evaluating for CAA or amyloid-related imaging abnormalities (ARIA). Postcontrast MRI may be frequently ordered for evaluation of rapidly progressive cognitive decline, with potential etiologies that may include neoplastic, infectious, toxic-metabolic, or autoimmune disorders.[18] However, the most common type of MRI recommended is without IV contrast, according to the American College of Radiology guidelines.[12] Thus, a common pitfall to avoid when ordering imaging for dementia is the use of IV contrast unless a suspected etiology may warrant the use of contrast, such as those for rapidly progressive dementias. Discordance between image interpretation and clinical evaluation can be minimized by (1) evaluation of a chronically progressive versus rapidly progressive development of dementia, (2) the presence of fluid biomarkers, and (3) understanding of potential comorbidities that may occur with common dementias such as AD and vascular disease. Clinical communication between neurologists and neuroradiologists remain important in facilitating the diagnostic process.

## MRI SAFETY CONSIDERATIONS

When scanning people in late life, the main consideration for neurologists and neuroradiologists is the safety of scanning with the various medical devices a patient may have. The main example found in clinical practice is a pacemaker, but the variety of devices has expanded and includes cochlear implants and orthopedic hardware. Thus, when considering whether to request a brain MRI in a person with any medical hardware, it is essential that the neurologist consult with the neuroradiologist about the device and its MRI compatibility. The neuroradiologist then must consider several factors. First, if no documentation exists on the MRI compatibility or incompatibility of the device, MRI should not be performed because the risk is unknown. If prior medical documentation is available noting that the device requires no specific conditions for MRI, the scan can be performed. If specific conditions are documented by the manufacturer, the conditions can be viewed on a central common website (mrisafety.com), which provides ratings of MRI safety as defined by the US Food and Drug Administration (FDA): MRI Safe, MRI Unsafe, and MRI Conditional. Patients with devices rated MRI Unsafe should not undergo MRI examinations. Patients with devices designated as MRI Safe can be scanned. Patients with devices rated as MRI Conditional devices may be scanned only if specific conditions are met. MRI Conditional devices are further rated as Conditional 1 through Conditional 8, with specific considerations noted for each rating

(mrisafety.com/Terminology.html). With some MRI safety policies, MRI Conditional 4 and MRI Conditional 5 ratings may warrant scanning done by a certified magnetic resonance safety officer as these conditions are particularly manufacturer specific. Such cases are typically urgent or emergent clinical situations in which the risks of the scan must be weighed against the clinical benefit. Clinical collaboration between the neurologist and neuroradiologist is essential in the decision-making process. In some circumstances, the neuroradiologist may also consult with an MRI physicist to further determine MRI safety. Neurologists should familiarize themselves with the MRI safety categories and related documentation of devices to best inform their neuroradiology MRI safety consultations.

KEY POINTS

- If specific conditions for use of MRI in patients with medical devices are documented by the device manufacturer, the conditions can be evaluated on mrisafety.com.
- When evaluating brain MRIs from a neuroradiologic perspective, is it important to consider whether the dementia under evaluation is chronically progressive or rapidly progressive.

## CHRONICALLY PROGRESSIVE AND RAPIDLY PROGRESSIVE DEMENTIAS

When evaluating brain MRIs from a neuroradiologic perspective, is it important to consider whether the dementia under evaluation is chronically progressive or rapidly progressive. Chronically progressive dementias, such as AD, frontotemporal dementia (FTD), and dementia with Lewy bodies (DLB), typically develop insidiously over months to years.[19] Vascular dementia may have an acute onset commensurate with the occurrence of stroke and then not progress until and unless additional vascular insults occur. In contrast, the rapidly progressive dementias typically develop over weeks to months. Rapidly progressive dementias can have a wide variety of causes, ranging from vascular to toxic/metabolic, infectious, and systemic causes; heavy metal poisoning; autoimmune diseases; and neoplastic processes. This article focuses on chronically progressive dementias and the use of quantitative MRI volumetrics as a practical clinical aid to dementia diagnosis.

## APPLICATION OF NEUROIMAGING TO DEMENTIA

This section will overview the use of volumetric quantification techniques on brain MRI for dementia.

### Brain Atrophy Quantification With MRI Volumetrics

AD is the most common cause of dementia, with longitudinal brain MRI revealing progressive atrophy in the hippocampal, temporal, and parietal regions. Jack and colleagues[20] determined that the normal age-related annualized hippocampal atrophy rate is 1.73% from a cubic millimeter unit of measurement of hippocampal volume. With early symptomatic AD (eg, mild cognitive impairment due to AD),[21] this annual rate is increased to 2.5% and rises with greater AD dementia severity.[20,22] Another study by Fotenos and colleagues[23] noted whole-brain atrophy rates of 0.45% in cognitively normal individuals and 0.98% per year in individuals with AD. Brain atrophy begins around age 30 and progresses throughout the lifespan.[24] From 30 to 80 years of age, humans experience frontal lobe volume loss of 14% and hippocampal volume loss of 13%.[25] The same study found that white matter volume in particular shrinks, with a 24% loss of volume in the frontal lobe and the majority of this loss occurring after the age of 70.[25] However it is important to note that many so-called normative older cohorts included individuals with preclinical AD, so truly normal aging may not be affected as greatly by atrophy as the literature might indicate.

Tracking these structural changes is enabled by volumetric quantification on brain MRI. Although this can be done with research software programs,[26-28]

FDA-cleared software programs also exist and are shown alongside research software programs in TABLE 7-1[29-40].[41]

Automated volumetric analysis programs, whether FDA cleared or research based, are readily available both nationally and globally and are increasingly being used. Many are accessible through Health Insurance Portability and Accountability Act (HIPAA)–compliant web portals, increasing the range of access. The average turnaround time for FDA-cleared programs ranges from 10 minutes on a web portal to contemporaneous with images as they are acquired on MRI scanners. One FDA-cleared program processed 115,000 clinical brain MRIs from 2006 to 2016.[42] Additionally, the applications demonstrated in peer-reviewed literature have expanded from dementia[29] to multiple sclerosis,[43] traumatic brain injury,[44] and mesial temporal sclerosis.[45] The cost of such programs is modest.[9] An ordering neurologist can specify a request for volumetric quantification in their ordering comments if the electronic medical record lacks this option. Automated volumetrics agree with manual volumetry, with one study of an FDA-cleared program showing average Dice similarity coefficients (a similarity metric) of between 86% and 88% in hippocampal measurements across cognitively normal controls, prodromal AD, and AD dementia in the Alzheimer Disease Neuroimaging Initiative (CASE 7-1).[30] Automated volumetry demonstrates a high degree of accuracy in detecting brain atrophy related to a clinical diagnosis of dementia, with another FDA-cleared volumetric program showing accuracy of 99%.[31] Additionally, automated volumetry can detect both cross-sectional and longitudinal atrophy that can be missed on conventional visual reads (CASE 7-2).[48,49] It is important to note that hippocampal volume loss is not specific for AD as it has been observed in other

TABLE 7-1 **Software Programs Available for Automated Volumetric Analysis**

**US Food and Drug Administration (FDA)–cleared magnetic resonance volumetric software**

- NeuroQuant (cortechs.ai/products/neuroquant)[29]
- Neuroreader (brainreader.net)[30]
- Icometrix (icometrix.com)[31]
- Quantib (quantib.com)[32]
- CorticoMetrics (corticometrics.com)[33]
- Siemens Brain Morphometry (magnetomworld.siemens-healthineers.com/clinical-corner/clinical-talks/brain-morphometry.html)[34]

**Research magnetic resonance volumetric software**

- FreeSurfer (surfer.nmr.mgh.harvard.edu)[35]
- Voxel-based morphometry (dbm.neuro.uni-jena.de)[36]
- volBrain (volbrain.upv.es)[37]
- Brain MRICloud (mricloud.org)[38]
- FastSurfer (deep-mi.org/research/fastsurfer)[39]
- FSL (fsl.fmrib.ox.ac.uk/fsl/fslwiki)[40]

conditions, including in relation to traumatic brain injury,[50] mesial temporal sclerosis,[45] and hippocampal sclerosis of aging.[51] Normal volumetric findings on brain MRI, however, do not exclude AD dementia (CASE 7-3).

Brain atrophy related to neurodegenerative dementing diseases is progressive in nature and worsens over time. By this rationale, brain volumes that are technically within a "normal" range when compared to a normal database, but worsening over time, may suggest progressive atrophy related to neurodegeneration even if still within the "normal" range (FIGURE 7-5). In other words, a decline in regional brain volume even within a statistically normal comparative range can be compatible with progressive brain atrophy in the setting of neurodegenerative disease.

In summary, longitudinal brain quantification in the workup of dementia can improve both the sensitivity of the workup and confidence in support of the underlying diagnosis. Brain atrophy can be detected with intervals as short as 6 months,[53] but the majority of studies track atrophy over 1 year.[54]

### Molecular Imaging Studies in Dementia

The relatively recent amyloid, tau, neurodegeneration (A/T/N) framework for AD research[55] may also offer some insights into the diagnostic imaging evaluation of dementia. In this framework, *A* stands for the amyloid found in the amyloid plaques of AD that can be identified with amyloid PET and/or CSF or plasma biomarker evaluations. *T* stands for tau identified in neurofibrillary tangles that can also be noted on tau PET and/or fluid biomarker sampling. Although tau PET agents, including flortaucipir F 18, have been important in ongoing investigations of AD pathology,[56,57] the clinical use of tau PET scans has yet to be defined. Currently, tau PET holds promise as a surrogate marker for monitoring drug treatment response in clinical trials. It also can potentially identify different AD clinical phenotypes.[58] Although first-generation tau tracers in some instances were limited by off-target binding, newer tracers avoid these pitfalls and can potentially track different patterns of tau deposition in other neurodegenerative diseases, such as corticobasal degeneration and progressive supranuclear palsy.[59] *N* stands for neurodegeneration, the correlates of which on imaging include brain atrophy on MRI or glucose hypometabolism on FDG-PET.[60] The A/T/N framework is being examined in research settings, but in clinical practice, physicians caring for patients with dementia are most likely to monitor the *N* component using brain MRI and/or FDG-PET. Brain MRI characterizes the anatomic specificity and extent of neurodegeneration.

The current FDA-cleared amyloid PET tracers are florbetapir, florbetaben, and flutemetamol. These tracers have similar standards of visual interpretation, with comparable sensitivity for detecting amyloid deposition ranging between 87.2% and 91.7%.[61] Each of these tracers can be requested by a practicing neurologist based on their FDA clearance. However, given the lack of coverage by the Centers for Medicare & Medicaid Services, the clinical availability of both amyloid and tau PET tracers is limited by individual patient ability to pay. The cost of an amyloid PET scan can be prohibitive.[9]

Standard clinical interpretations of such scans are focused on grayscale images, and thus color scales are not required for this purpose but are used for one of the current FDA-cleared tracers, flutemetamol F 18, to provide an

**KEY POINTS**

- Brain atrophy related to neurodegenerative dementing diseases is progressive in nature and worsens over time.
- A decline in regional brain volume even within a statistically normal comparative range can be compatible with progressive brain atrophy in the setting of neurodegenerative disease.
- The relatively recent amyloid, tau, neurodegeneration (A/T/N) framework for AD research may offer some insights into the diagnostic imaging evaluation of dementia.
- The amyloid, tau, neurodegeneration (A/T/N) framework is being examined in research settings, but in clinical practice, physicians caring for patients with dementia are most likely to monitor the N (neurodegeneration) component using brain MRI and/or fludeoxyglucose positron emission tomography (FDG-PET).
- The current US Food and Drug Administration–cleared amyloid positron emission tomography tracers are florbetapir, florbetaben, and flutemetamol.

## CASE 7-1

**An 80-year-old woman presented with a 2-year history of insidious-onset memory loss, perseverative behaviors, inattention, and irritability. The patient was a retired corporate officer. Her medical history was notable only for hypertension. Her blood pressure at time of evaluation was 171/88 mm Hg. Her Clinical Dementia Rating (CDR)[46] was 0.5, indicating very mild dementia.**

**The diagnostic considerations included Alzheimer disease (AD) as well as small vessel disease and vascular dementia, although the insidious course argued against a vascular cause. Brain MRI was obtained, which showed mild-appearing hippocampal volume loss (FIGURE 7-1A), minimal T2/fluid-attenuated inversion recovery (FLAIR) hyperintensities (FIGURE 7-1B), and no findings of basal ganglia/thalamic microbleeds from hypertension or cortical microbleeds suggestive of cerebral amyloid angiopathy (FIGURE 7-1C). Volumetric brain MRI quantification showed abnormally low hippocampal volumes (FIGURES 7-2A and 7-2B), higher lateral ventricular volumes (FIGURE 7-2C), and normal range parietal lobe thickness (FIGURE 7-2D).**

### COMMENT

The clinical interpretation of the patient's MRI precluded hypertensive vascular disease as the primary factor behind the patient's dementia given the lack of white matter hyperintensities or microbleeds to indicate end organ damage from chronic vascular disease. The mild hippocampal volume loss suggested AD. Hippocampal volumes have been identified as 17% smaller in people who subsequently develop AD dementia compared with people who remain cognitively normal 2 to 3 years later.[47] FIGURE 7-2 shows that the quantified hippocampal volumes in this patient are at the first percentile when compared to a normal database, signifying more than 2 standard deviations from the mean. Note that the figure shows ventricular and parietal lobe volumes within 2 standard deviations of the mean of the normal database. Temporal lobe cortical thickness, not shown, was between 1 and 2 standard deviations from the mean. Thus, the quantified low hippocampal volumes were the most sensitive metrics of brain abnormality in this patient with mild dementia and the clinical read of hippocampal atrophy. In the context of the hippocampal findings, the lateral ventricular volumes and parietal lobe thickness, although technically within 2 standard deviations from the mean, may also be abnormal. These findings further illustrate added value of quantified brain volumes with statistical comparisons to normal data.

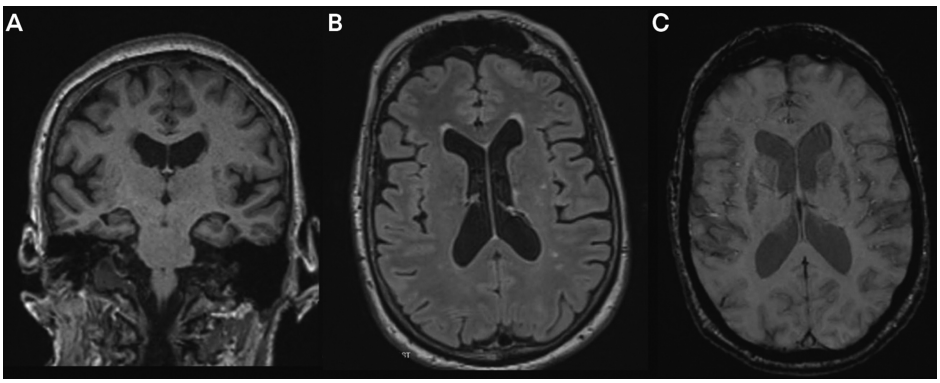


**FIGURE 7-1**

Imaging of the patient in CASE 7-1. *A*, Coronal T1-weighted MRI shows mild-appearing hippocampal volume loss. *B*, Axial fluid-attenuated inversion recovery (FLAIR) MRI shows mild small vessel ischemic disease. *C*, Axial susceptibility-weighted imaging (SWI) MRI shows lack of cerebral microbleeds.

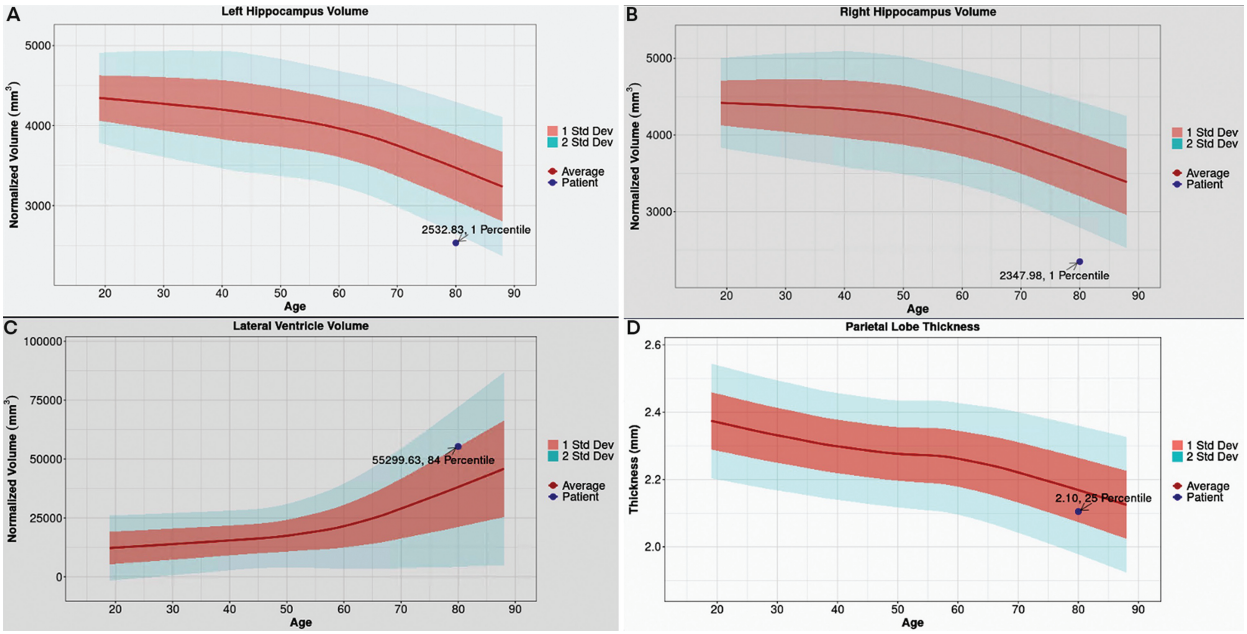


**FIGURE 7-2**

Volumetric MRI findings for the patient in CASE 7-1. Volumetric brain MRI quantification findings show abnormally low left (*A*) and right (*B*) hippocampal volumes and higher lateral ventricular volumes (*C*) and normal range parietal lobe thickness (*D*).

## CASE 7-2

**A 69-year-old man presented with a 2-year history of the gradual onset and progression of memory loss and behavioral changes. He no longer recognized people he previously knew well, purchased unneeded items, and had experienced personality changes.**

**Initial neuroimaging evaluation done at this initial visit after 2 years of progressive decline showed brain volumes within 2 standard deviations of the mean, hence within the normal range. However, follow-up volumetric quantification 2 years later revealed volumetric declines in frontal and temporal lobe thickness and in hippocampal volume at rates higher than expected in normal aging (FIGURE 7-3); he was ultimately clinically diagnosed with frontotemporal dementia.**

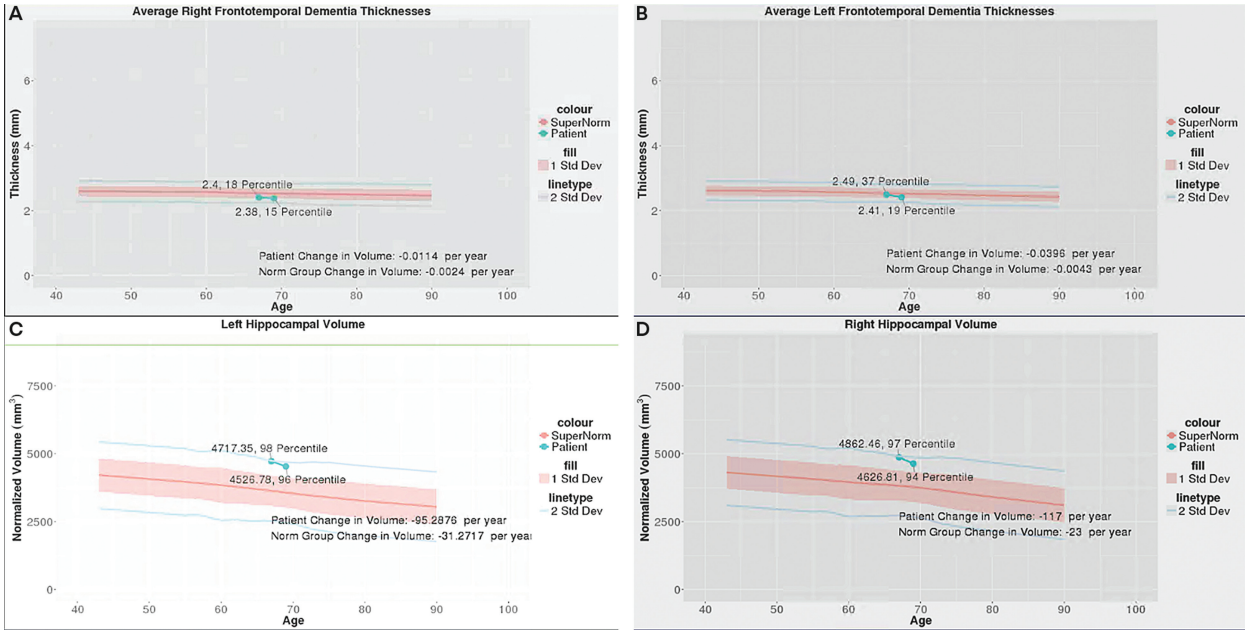


**FIGURE 7-3**

**Volumetric brain MRI quantification findings of the patient in CASE 7-2. The top two panels show longitudinally reduced frontotemporal thickness on both the right (*A*) and left (*B*) sides. The bottom panels (*C*, *D*) show longitudinally decreased hippocampal volumes.**

**COMMENT**

This case emphasizes the utility of longitudinal imaging in frontotemporal dementia as well as Alzheimer disease dementia by showing the progressive loss of frontal and temporal lobe thickness. This case also highlights the additional sensitivity conveyed with cortical thickness measurements in addition to volumes.

## CASE 7-3

**A 67-year-old woman presented with a 1-year history of cognitive decline, including repetition of questions and stories, forgetting details, omitting ingredients from a recipe, and increasingly low tolerance to stress.**

**Brain MRI volumetric quantifications, including hippocampal volumes, were all in the normal range of within 2 standard deviations from the control mean. However, a brain amyloid positron emission tomography (PET) obtained as part of a research study showed brain amyloidosis consistent with underlying AD pathology (FIGURE 7-4), with cortical[52] florbetapir F 18 uptake in the gray matter distributed out to the periphery with concurrent loss of gray-white matter contrast.**

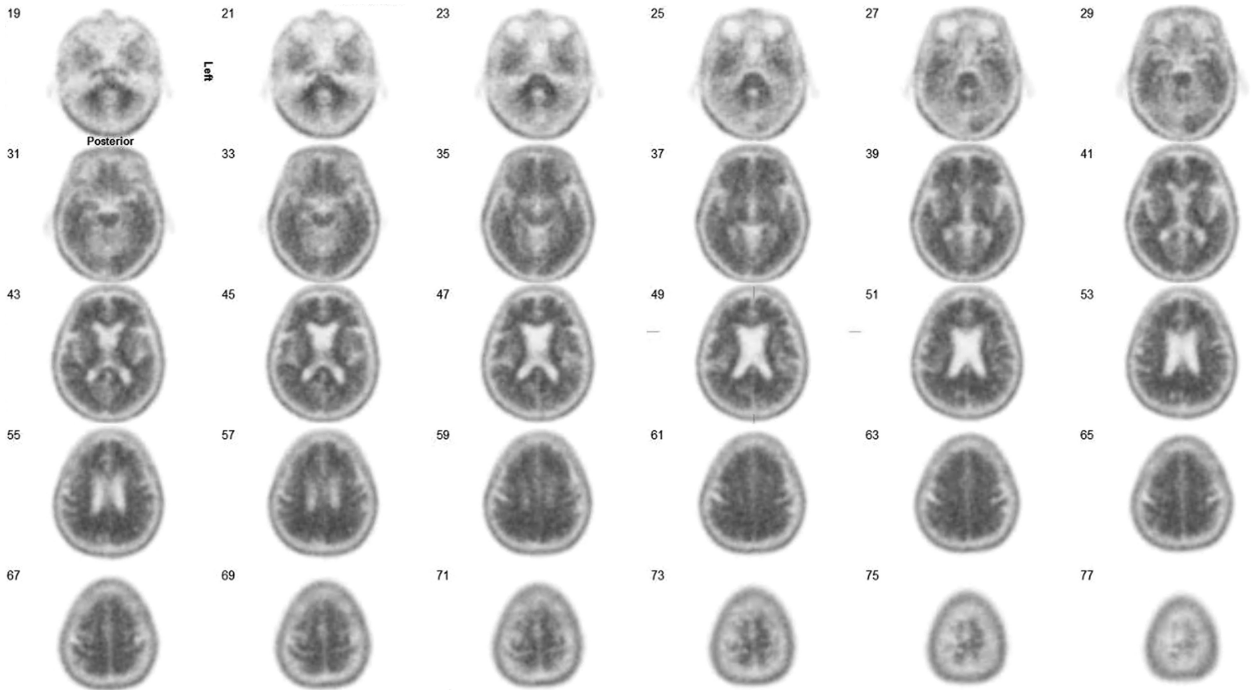


**FIGURE 7-4**
**Example of a positive brain amyloid positron emission tomography (PET) scan in a person with normal range quantified brain volumes, including hippocampal volumes. The *darker shades of gray* areas show increased amyloid uptake in supratentorial regions; *gray* areas in the cerebellum show the comparative lack of amyloid binding.**

**COMMENT**

In this case, the patient had normal-range derived MRI brain volumes, including in the hippocampus. However, further PET imaging revealed amyloid-positive binding indicative of underlying Alzheimer pathology.

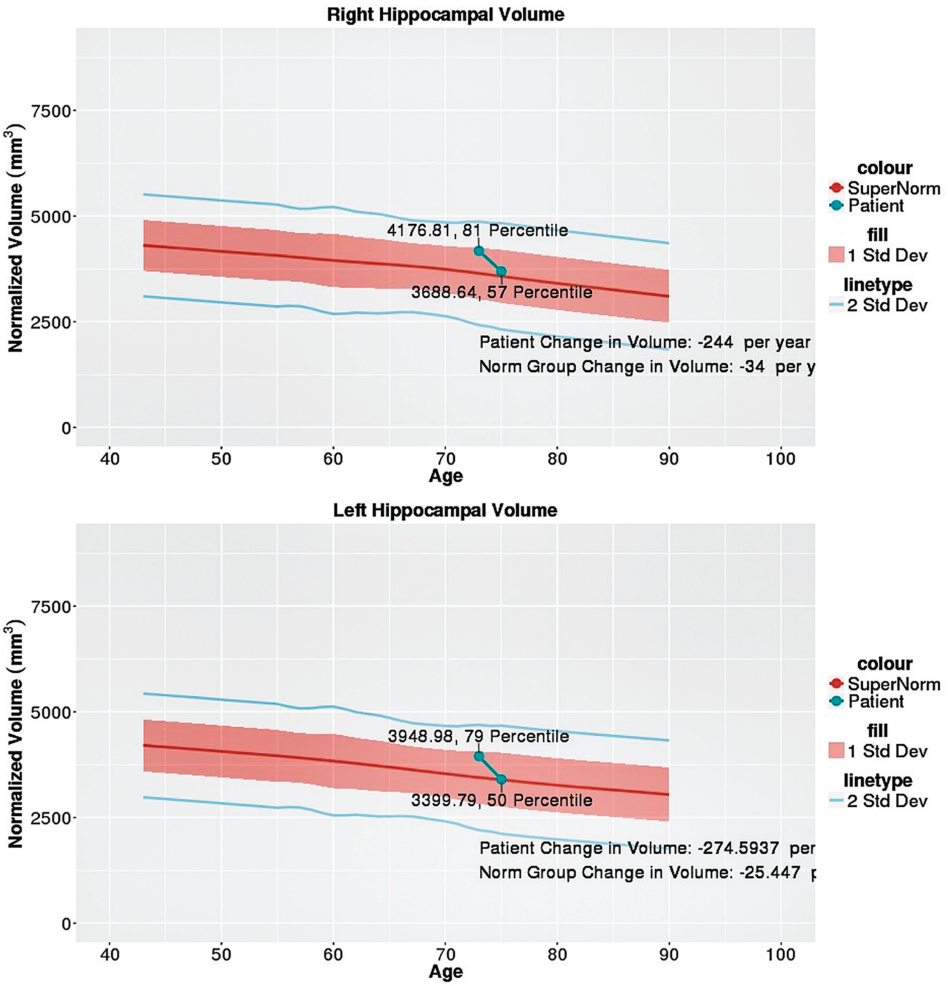


**FIGURE 7-5**

**A 75-year-old man presented with several years of subjective memory symptoms but no diagnosed dementia. The longitudinal volumetric findings in this individual showed increased hippocampal volume loss over a 2-year period beyond what is expected for normal aging, suggesting a dementia neurodegenerative process.**

improved ability to visually identify the progression of low to high intensity.[52] Although visual analysis is the current standard in amyloid PET image interpretation, standardized uptake value ratios (SUVRs) with a reference region such as the cerebellum can generate high diagnostic accuracy. The cerebellum is the most commonly used reference region for SUVR calculations because of the very low to no amyloid-β in the cerebellar gray matter and white matter, respectively.[62] One study found using SUVR with the cerebellum as a reference region generated an area under the curve of 93.5%.[63] Use of machine learning further improves upon this accuracy.[64] The IDEAS (Imaging Dementia—Evidence for Amyloid Scanning) study showed that use of amyloid PET changed management in more than 60% of cases with very mild and mild dementia, more than twice what the study predicted.[65]

Brain FDG-PET images show glucose metabolism, and hypometabolism is frequently seen in dementia.[60] This method may be useful in differentiating

between FTD and AD because of the characteristic temporoparietal hypometabolism in AD compared to the predominant frontal hypometabolism in behavioral variant FTD.[66] This distinction has high diagnostic utility, with one study showing sensitivity of 86% and specificity of 97.6% in evaluating 31 individuals with pathologically confirmed AD and 14 individuals with FTD.[66] The distribution of FDG-PET changes can suggest other neurodegenerative conditions, especially when postprocessed with z score maps (FIGURE 7-6).[67] Such processing can be done with FDA-cleared software tailored for FDG-PET brain analysis[68] in addition to visual reads. As the imaging abnormalities seen on FDG-PET can substantially overlap across different types of neurodegeneration, the use of more specific amyloid and tau biomarker studies will remain important to utilize as clinical practice evolves.

Much interest exists in the development of fluid and, in particular, plasma biomarkers for the detection of AD,[69,70] which have been shown to predict brain amyloidosis on PET.[71] Such work is essential as these tests will be needed to demonstrate biomarker positivity in individuals with suspected AD who are being evaluated for possible anti-amyloid therapy and have substantially lower costs than PET. Although amyloid and tau PET demonstrate the full anatomic distribution of these biomarkers, patient access to PET scanners is not ubiquitous. Thus, plasma biomarkers will remain important for maximizing this access to determine eligibility for anti-amyloid therapy.

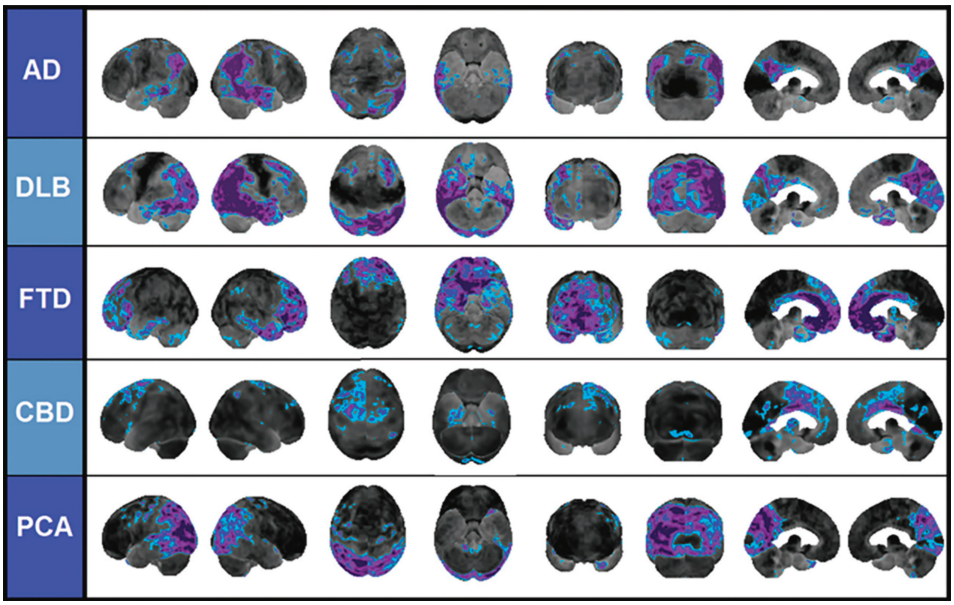


**FIGURE 7-6**

**Differential patterns of hypometabolism on fludeoxyglucose positron emission tomography (FDG-PET) z score maps in neurodegenerative disease with temporal parietal hypometabolism in Alzheimer disease (AD), increased occipital hypometabolism in dementia with Lewy bodies (DLB), frontal dominant hypometabolism in frontotemporal dementia (FTD), asymmetry in corticobasal degeneration (CBD), and posterior dominant cortical hypometabolism in posterior cortical atrophy (PCA). The *blue* and *purple* colors denote areas of the FDG-PET scan that are lower than -2 standard deviations from the mean of the control comparison population.**

Reprinted with permission from Brown RKJ, et al, RadioGraphics.[67] © 2014 Radiological Society of North America.

**KEY POINTS**

- **Although visual analysis is the current standard in amyloid positron emission tomography image interpretation, standardized uptake value ratios with a reference region such as the cerebellum can generate high diagnostic accuracy.**
- **The distribution of FDG-PET changes can suggest other neurodegenerative conditions, especially when postprocessed with z score maps.**
- **As the imaging abnormalities seen on FDG-PET can substantially overlap across different types of neurodegeneration, the use of more specific amyloid and tau biomarker studies will remain important to utilize as clinical practice evolves.**
- **Much interest exists in the development of fluid and, in particular, plasma biomarkers for the detection of AD, which have been shown to predict brain amyloidosis on PET.**

### White Matter Hyperintensities

The role of chronic hypertensive vascular disease as an etiologic factor for cognitive decline is best evaluated on FLAIR images, which can demonstrate abnormally high signal in the white matter known as white matter hyperintensities or white matter lesions.[72] The distribution of such lesions in the setting of chronic small vessel ischemic changes is typically in periventricular or subcortical regions or in the deep white matter, and the location of these lesions in older people supports the underlying small vessel ischemic etiology[73] and can independently predict brain atrophy.[74] On histopathology, these lesions signify underlying vascular disease, including cerebral infarcts, lacunes, and subcortical arteriosclerotic leukoencephalopathy.[75] Grading the magnitude of such changes as mild, moderate, or severe is done with the Fazekas scale,[72] which provides a simple visual scale of white matter lesion severity (FIGURE 7-7). As the severity of white matter disease increases, so too does the confluence of the lesions, mainly in a periventricular distribution. Additional lesions in subcortical and deep white matter would demonstrate an increasingly cloudlike appearance.

### Cerebral Microbleeds

Cerebral microbleeds manifest as focal round areas of reduced signal on susceptibility-sensitive sequences, such as SWI on 3.0T and gradient recalled echo (GRE) on 1.5T systems. Three or more of these lesions confer a higher risk of cognitive impairment.[76] However, cerebral microbleeds have several etiologies, and these different causes can be suggested by the spatial distribution of these lesions (FIGURE 7-8).[77] Differentiating between these findings is important as the bleeding risk as evidenced by the development of lobar hemorrhage in CAA is high, ranging from 3.9% to more than 11% with the presence of cortical superficial siderosis (deposition of chronic blood product over the cerebral convexities).[78] Cerebral microbleeds are abnormal accumulations of hemosiderin in blood vessels, and with hypertension this is presumed to be due to endothelial cell damage and related inflammation.[77] This commonly happens in the basal ganglia because of the vulnerability of the supplying medial lenticulostriate arteries to chronic hypertension.[79] With traumatic brain injury, this is

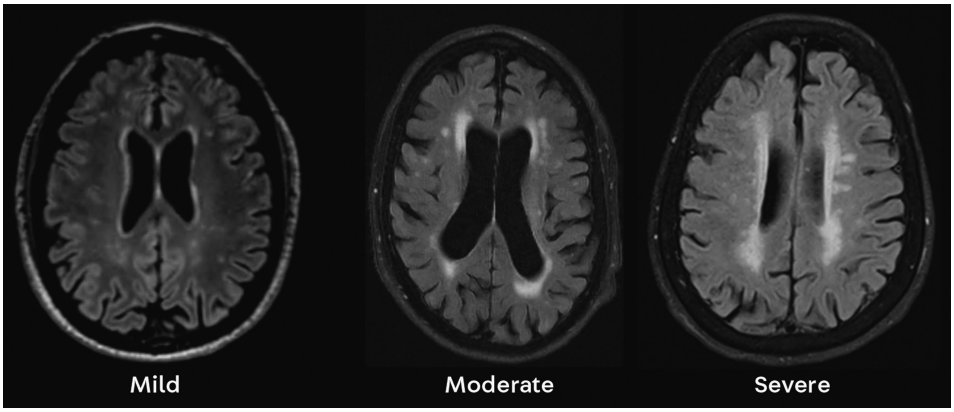


**FIGURE 7-7**
**Fazekas white matter grade (mild, moderate, severe) for small vessel ischemic disease.**

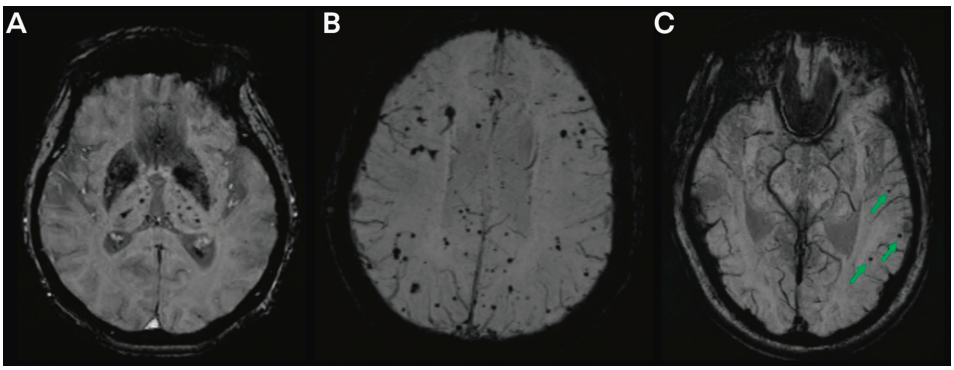


**FIGURE 7-8**

**Examples of different etiologies of cerebral microbleeds suggested by spatial distribution. Axial susceptibility-weighted imaging (SWI) shows the typical location of hypertensive microbleeds in the bilateral thalamus and basal ganglia (*A*), bilateral cortically distributed microbleeds common in cerebral amyloid angiopathy, often further characterized by large lobar microhemorrhage (*not shown*) in 8.5% of patients with cerebral amyloid angiopathy[62] (*B*), and three asymmetric left temporal lobe microbleeds in a patient with a history of traumatic brain injury (*C*, *arrows*).**

secondary to diffuse axonal injury in which hemosiderin-filled macrophages next to small vessels are related to prior extravasation of blood[80]; this frequently asymmetrically affects frontal and temporal lobes as these are frequent areas of injury.[81] In CAA, cerebral microhemorrhages relate to amyloid-β deposition and insoluble amyloid fibrils within the walls of leptomeningeal and cortical arterioles.[82]

### Brain MRI in Amyloid-related Imaging Abnormalities

Brain MRI is essential for the recently approved anti-amyloid therapy with aducanumab to monitor for the complications of amyloid-related imaging abnormalities with hemorrhage and superficial siderosis (ARIA-H) or with vasogenic edema with or without sulcal effusion (ARIA-E).[83] These findings are collectively seen in up to 35% of individuals treated with aducanumab, which as of January 11, 2022, has been approved by the Centers for Medicare & Medicaid Services for coverage with evidence development.[84,85] Monitoring for these complications in the clinical trials for aducanumab occurred at baseline or within 1 year of starting treatment, after the seventh infusion (first dose of 10 mg/kg), and after the twelfth infusion (sixth dose of 10 mg/kg). The ARIA classification criteria from the aducanumab FDA label are listed in TABLE 7-2.[86] FIGURE 7-9 shows examples of ARIA-H and ARIA-E.

### Dementia With Lewy Bodies

DLB refers to a syndrome characterized neuropathologically by the abnormal aggregation of α-synuclein,[87] an abundant 140-amino acid neuronal protein seen mainly in the neuronal presynaptic terminal. Clinically it is identified by progressive cognitive decline that often involves executive and visuospatial dysfunction.[88] On imaging, a biomarker suggestive of DLB is ioflupane I 123, which labels the dopamine transporter in the nigrostriatal dopaminergic pathway on PET or single-photon emission computed tomography (SPECT). Reduced

**KEY POINTS**

- **The role of chronic hypertensive vascular disease as an etiologic factor for cognitive decline is best evaluated on fluid-attenuated inversion recovery images.**
- **The distribution of white matter hyperintensities in the setting of chronic small vessel ischemic changes is typically in periventricular or subcortical regions or in the deep white matter, and the location of these lesions in older people supports the underlying small vessel ischemic etiology and can independently predict brain atrophy.**
- **In cerebral amyloid angiopathy, cerebral microhemorrhages relate to amyloid-β deposition and insoluble amyloid fibrils within the walls of leptomeningeal and cortical arterioles.**
- **Brain MRI is essential for the recently approved anti-amyloid therapy with aducanumab to monitor for the complications of amyloid related imaging abnormalities with hemorrhage and superficial siderosis (ARIA-H) or with vasogenic edema with or without sulcal effusion (ARIA-E).**
- **On imaging, a biomarker suggestive of dementia with Lewy bodies is ioflupane I 123, which labels the dopamine transporter in the nigrostriatal dopaminergic pathway on PET or single-photo emission computed tomography (SPECT).**

binding of ioflupane I 123 in the basal ganglia on a dopamine transporter scan reflects abnormally low presynaptic dopamine. This finding, in turn, relates to loss of dopaminergic neurons that can occur in DLB,[89] Parkinson disease,[90] multiple system atrophy,[91] progressive supranuclear palsy,[91] and corticobasal degeneration.[92] Given the overlapping findings, an abnormal ioflupane I 123 dopamine transporter scan does not establish a specific diagnosis of DLB but can be an indicative biomarker when other clinical information is supportive of the diagnosis. One systematic review found that dopamine transporter scans change management in 54% of cases and resulted in a change in diagnosis in 31% of cases.[93] FIGURE 7-10 shows examples of normal and abnormal dopamine transporter scans.

### Normal Pressure Hydrocephalus

Normal pressure hydrocephalus (NPH), classically consisting of the clinical triad of gait dysfunction, urinary incontinence, and dementia, is a differential diagnostic consideration in some patients with dementia. MRI findings suggestive of NPH include ventriculomegaly out of proportion to sulcal dilatation (FIGURE 7-11A), as evidenced by a reduced callosal angle[94] (FIGURE 7-11B) and tenting of the lateral ventricle (FIGURE 7-11C) with a CSF flow void in the cerebral aqueduct (FIGURE 7-11D). The callosal angle is drawn at the posterior commissure on coronal T1-weighted MRIs; it is typically abnormal in the setting of NPH when it is between 50 and 80 degrees and typically normal when it is between 100 and 120 degrees.[94] Tenting of the lateral ventricle is seen from the communicating hydrocephalus of NPH, but the finding is not exclusive to this disorder. This is also true with increased CSF flow manifesting as a cerebral aqueduct flow void.

Although the clinical management of NPH does not always yield positive outcomes and ventricular shunting can have complication rates of up to 35%,[95]

TABLE 7-2 **ARIA Classification Criteria for Aducanumab[a]**

| | Radiographic severity | | |
|---|---|---|---|
| **ARIA type** | **Mild** | **Moderate** | **Severe** |
| **ARIA-E** | Fluid-attenuated inversion recovery (FLAIR) hyperintensity confined to sulcus and/or cortex/subcortical white matter in one location <5 cm | FLAIR hyperintensity 5 to 10 cm or more than one site of involvement, each measuring <10 cm | FLAIR hyperintensity measuring >10 cm, often with significant subcortical white matter and/or sulcal involvement; one or more separate sites of involvement may be noted |
| **ARIA-H microhemorrhage** | ≤4 new incident microhemorrhages | 5 to 9 new incident microhemorrhages | 10 or more new incident microhemorrhages |
| **ARIA-H superficial siderosis** | 1 focal area of superficial siderosis | 2 focal areas of superficial siderosis | >2 focal areas of superficial siderosis |

ARIA = amyloid-related imaging abnormalities; ARIA-E = amyloid-related imaging abnormalities with vasogenic edema with or without sulcal effusion; ARIA-H = amyloid-related imaging abnormalities with hemorrhage and superficial siderosis.
[a] Reprinted from the US Food and Drug Administration.[86]

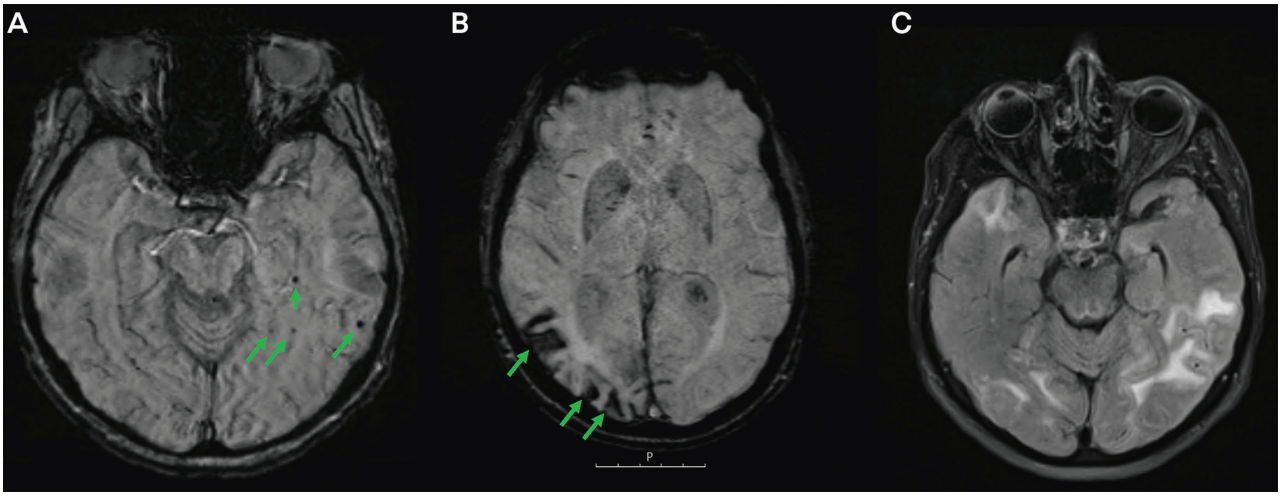


**FIGURE 7-9**
**Examples of amyloid-related imaging abnormalities (ARIA). *A*, Axial susceptibility-weighted imaging (SWI) shows ARIA-H with cerebral microhemorrhages (*arrows*); *B*, Axial SWI shows the superficial siderosis that can be seen in ARIA-H and indicates hemosiderin staining on the pial surface of the brain (*arrows*); *C*, Axial imaging fluid-attenuated inversion recovery (FLAIR) image shows ARIA-E with multiple areas of edema.**

the question of NPH versus AD can be a diagnostic dilemma; however, volumetric quantification can be useful in resolving the dilemma. In FIGURE 7-12, the increased ventricular volume (99th percentile) and the comparison of ventricular to cerebral volume suggests ventriculomegaly out of proportion to brain atrophy. Lack of hippocampal atrophy for this amount of ventriculomegaly in the presence of suggestive clinical findings for NPH suggests

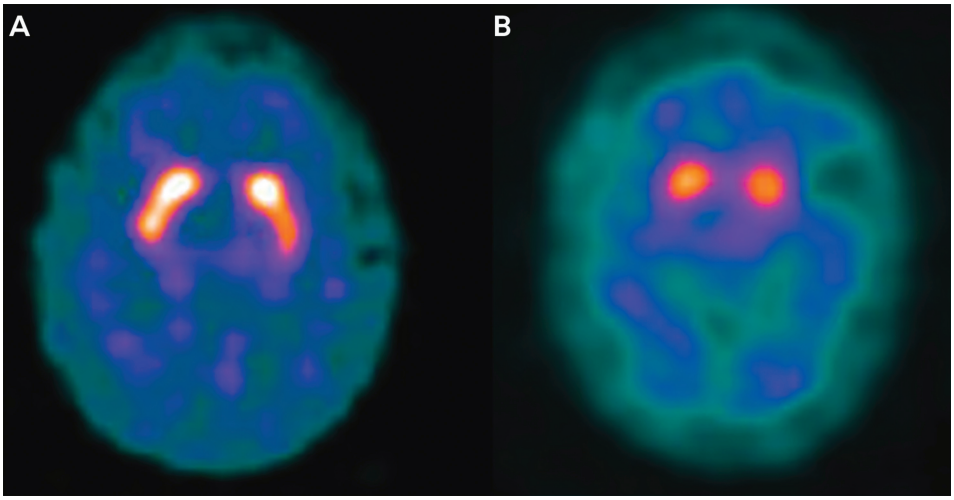


**FIGURE 7-10**
**Normal and abnormal dopamine transporter scans. *A*, Normal dopamine transporter scan shows dopamine uptake in the basal ganglia with a typical lentiform morphology. *B*, Abnormal dopamine transporter scan showing reduced dopamine uptake in the basal ganglia with a rounded shape. *Orange to white* intensity of color indicates increased dopamine uptake. *Blue to purple* intensity of colors denotes lack of dopamine uptake.**

KEY POINT

- The callosal angle is drawn at the posterior commissure; it is typically abnormal in the setting of normal pressure hydrocephalus when it is between 50 and 80 degrees and typically normal when it is between 100 and 120 degrees.

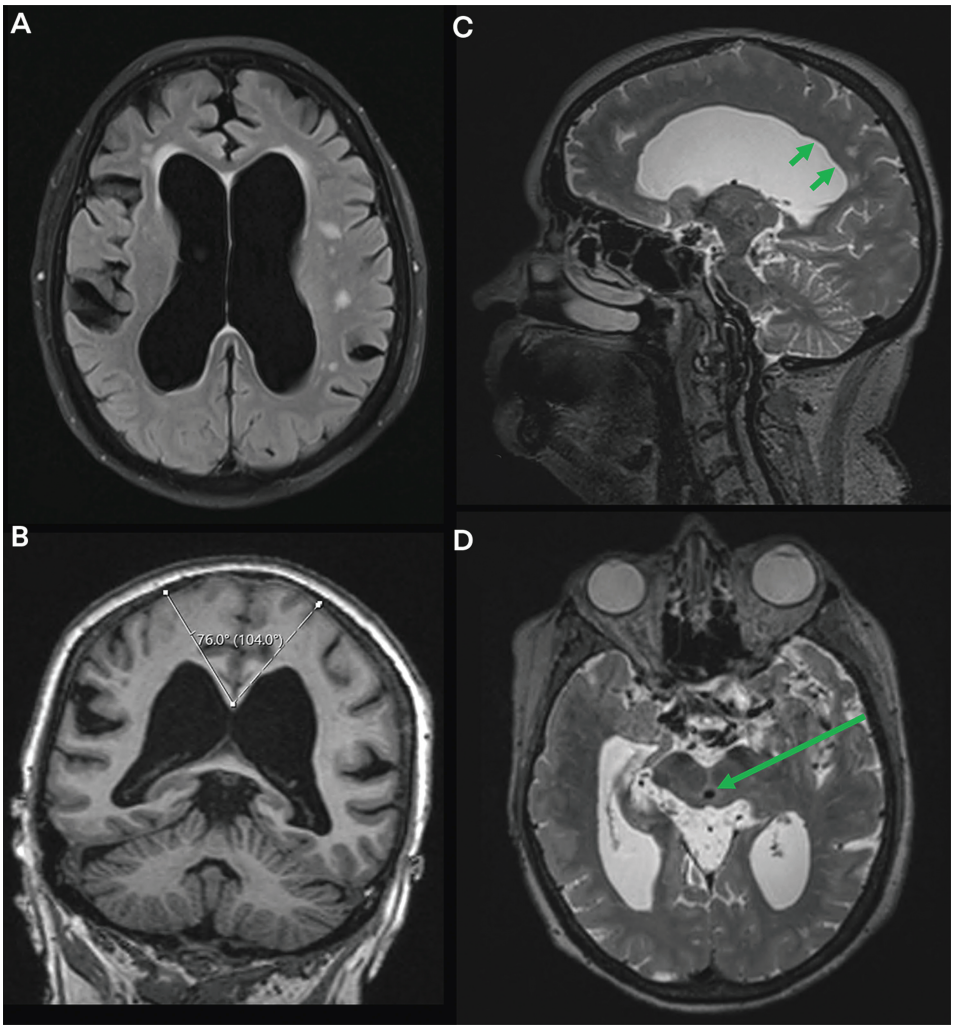


FIGURE 7-11

**MRI findings suggestive of normal pressure hydrocephalus in a patient who presented with falls, urinary incontinence, and memory loss. *A*, Axial fluid-attenuated inversion recovery (FLAIR) MRI shows ventriculomegaly out of proportion to sulcal dilatation. *B*, Coronal T1-weighted MRI shows a reduced callosal angle of 76 degrees. The callosal angle is measured at the level of the posterior commissure on a coronal image. In a patient with clinical features suggestive of normal pressure hydrocephalus, a callosal angle of 50 to 80 degrees is more suggestive of normal pressure hydrocephalus, whereas a callosal angle of 100 to 120 degrees is less suggestive of normal pressure hydrocephalus. *C*, Sagittal T2-weighted MRI shows tenting of the lateral ventricle (*arrows*). *D*, Axial T2-weighted MRI shows a CSF flow void in the cerebral aqueduct (*arrow*).**

that the clinical findings are more likely related to NPH rather than to AD dementia, although these pathologies can coexist.[96]

## CONCLUSION

The elements of neuroradiologic reporting are changing from historically focused reports that rule out structural causes of dementia. New reporting is now supplemented by quantification of regional brain volumes to characterize neuroimaging correlates of neurodegeneration. Additional semiquantitative

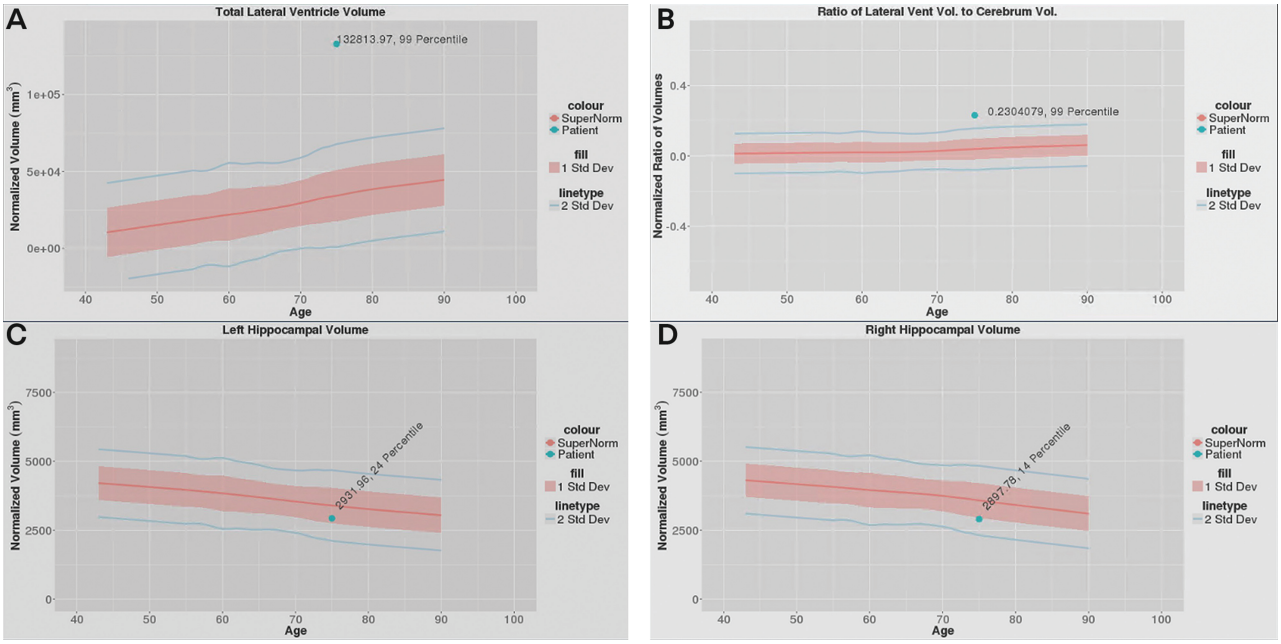


**FIGURE 7-12**

**Volumetric quantification findings in a case of normal pressure hydrocephalus show abnormally elevated ventricular volume out of proportion to cerebral volume (*A, B*) and relatively preserved hippocampal volume (*C, D*).**

imaging metrics of small vessel ischemic disease and cerebral microbleeds provide additional insights into other contributors to cognitive decline and dementia. All this information is obtainable from a single brain MRI that is already recommended in dementia evaluation. However, volumetric quantification, although readily available, has yet to be widely implemented and may require increased education and awareness among practicing clinicians. Additionally, further work must be done to combine available brain MRI information with other biomarkers from PET and fluid biomarkers to identify individuals at risk for dementia earlier in the disease process, thus allowing for increased effectiveness of risk reduction measures and new treatments.

## USEFUL WEBSITES

**ALZHEIMER'S DISEASE NEUROIMAGING INITIATIVE**
This website provides structural MRI protocols specific to device manufacturer.

adni.loni.usc.edu/methods/documents/mri-protocols

**MRISAFETY.COM**
This website provides information on MRI safety ratings for various devices and includes a reference manual, safety videos, and training information.

Mrisafety.com

**STANDARDIZED CENTRALIZED ALZHEIMER'S & RELATED DEMENTIAS NEUROIMAGING**
This website provides information on MRI and PET protocols for use in patients with Alzheimer disease and related dementias.

scan.naccdata.org

## REFERENCES


1 2020 Alzheimer's disease facts and figures. Alzheimers Dement 2020. doi:10.1002/alz.12068

2 Knopman DS, DeKosky ST, Cummings JL, et al. Practice parameter: diagnosis of dementia (an evidence-based review). Report of the Quality Standards Subcommittee of the American Academy of Neurology. Neurology 2001;56(9): 1143-1153. doi:10.1212/wnl.56.9.1143

3 Brito A, Tsang ACO, Hilditch C, et al. Intracranial dural arteriovenous fistula as a reversible cause of dementia: case series and literature review. World Neurosurg 2019;121:e543-e553. doi:10.1016/j.wneu.2018.09.161

4 Henderson JB, Zarghouni M, Hise JH, et al. Dementia caused by dural arteriovenous fistulas reversed following endovascular therapy. Proc (Bayl Univ Med Cent) 2012;25(4):338-340. doi:10.1080/08998280.2012.1192887

5 Enofe I, Thacker I, Shamim S. Dural arteriovenous fistula as a treatable dementia. Proc (Bayl Univ Med Cent) 2017;30(2):215-217. doi:10.1080/08998280.2017.11929592

6 Kincaid E. Want fries with that? A brief history of medical MRI, starting with a McDonald's. Forbes. Accessed April 13, 2022. forbes.com/sites/elliekincaid/2018/04/16/want-fries-with-that-a-brief-history-of-medical-mri-starting-with-a-mcdonalds

7 Magnetic Resonance. Chapter Twenty-One: Facts and figures. Accessed April 13, 2022. magnetic-resonance.org/ch/21-01.html

8 Weiner CJ. Seeing more with PET scans: scientists discover new way to label chemical compounds for medical imaging. News Center 2017. Accessed April 13, 2022. newscenter.lbl.gov/2017/07/27/new-chemistry-pet-scans-medical-imaging

9 Desikan RS, Rafii MS, Brewer JB, Hess CP. An expanded role for neuroimaging in the evaluation of memory impairment. AJNR Am J Neuroradiol 2013;34(11):2075-2082. doi:10.3174/ajnr.A3644

10 Statista. Average prices of a magnetic resonance imaging (MRI) in selected countries 2017. Accessed April 13, 2022. statista.com/statistics/312020/price-of-mri-diagnostics-by-country

11 McKhann GM, Knopman DS, Chertkow H, et al. The diagnosis of dementia due to Alzheimer's disease: recommendations from the National Institute on Aging-Alzheimer's Association workgroups on diagnostic guidelines for Alzheimer's disease. Alzheimers Dement 2011; 7(3):263-269. doi:10.1016/j.jalz.2011.03.005

12 Moonis G, Subramaniam RM. ACR appropriateness criteria - dementia. Revised 2019. Accessed April 13, 2022. acsearch.acr.org/docs/3111292/Narrative

13 Adduru V, Baum SA, Zhang C, et al. A method to estimate brain volume from head CT images and application to detect brain atrophy in Alzheimer disease. AJNR Am J Neuroradiol 2020;41(2): 224-230. doi:1.3174/ajnr.A6402

14 Health Quality Ontario. The appropriate use of neuroimaging in the diagnostic work-up of dementia: an evidence-based analysis. Ont Health Technol Assess Ser 2014;14(1):1-64.

15 Park M, Moon W-J. Structural MR imaging in the diagnosis of Alzheimer's disease and other neurodegenerative dementia: current imaging approach and future perspectives. Korean J Radiol 2016;17(6):827-845. doi:10.3348/kjr.2016.17.6.827

16 Haller S, Haacke EM, Thurnher MM, Barkhof F. Susceptibility-weighted imaging: technical essentials and clinical neurologic applications. Radiology 2021;299(1):3-26. doi:10.1148/radiol.2021203071

17 Ho AJ, Hua X, Lee S, et al. Comparing 3 T and 1.5 T MRI for tracking Alzheimer's disease progression with tensor-based morphometry. Hum Brain Mapp 2010;31(4):499-514. doi:10.1002/hbm.20882

18 Geschwind MD, Haman A, Miller BL. Rapidly progressive dementia. Neurol Clin 2007;25(3): 783-807, vii. doi:10.1016/j.ncl.2007.04.001.

19 Arvanitakis Z, Shah RC, Bennett DA. Diagnosis and management of dementia: review. JAMA 2019;322(16):1589-1599. doi:10.1001/jama.2019.4782

20 Jack CR, Petersen RC, Xu Y, et al. Rates of hippocampal atrophy correlate with change in clinical status in aging and AD. Neurology 2000; 55(4):484-489. doi:10.1212/wnl.55.4.484

21 Albert MS, DeKosky ST, Dickson D, et al. The diagnosis of mild cognitive impairment due to Alzheimer's disease: recommendations from the National Institute on Aging-Alzheimer's Association workgroups on diagnostic guidelines for Alzheimer's disease. Alzheimers Dement 2011; 7(3):270-279. doi:10.1016/j.jalz.2011.03.008

22 Jack CR, Shiung MM, Gunter JL, et al. Comparison of different MRI brain atrophy rate measures with clinical disease progression in AD. Neurology 2004;62(4):591-600. doi:10.1212/01.wnl.0000110315.26026.ef

23 Fotenos AF, Snyder AZ, Girton LE, et al. Normative estimates of cross-sectional and longitudinal brain volume decline in aging and AD. Neurology 2005;64(2):1032-1039. doi:10.1212/01.WNL.0000154530.72969.11

24 Peters R. Ageing and the brain. Postgrad Med J 2006;82(964):84-88. doi:10.1136/pgmj.2005.036665

25 Sherwood CC, Gordon AD, Allen JS, et al. Aging of the cerebral cortex differs between humans and chimpanzees. Proc Natl Acad Sci U S A 2011; 108(32):13029-13034. doi:10.1073/pnas.1016709108

26 Fischl B. FreeSurfer. Neuroimage 2012;62(2): 774-781. doi:10.1016/j.neuroimage.2012.01.021

27 Rugheimer SM, Liu Q, Sclabassi RJ, Sun M. Measurements with FreeSurfer. IEEE Trans Med Imag 2006;1:59-60.

28 Koenig LN, Day GS, Salter A, et al. Select atrophied regions in Alzheimer disease (SARA): an improved volumetric model for identifying Alzheimer disease dementia. NeuroImage Clin 2020;26:102248. doi:10.1016/j.nicl.2020.102248

29 Brewer JB. Fully-automated volumetric MRI with normative ranges: translation to clinical practice. Behav Neurol 2009;21(1):21-28. doi:10.3233/BEN-2009-0226

30 Ahdidan J, Raji CA, DeYoe EA, et al. Quantitative neuroimaging software for clinical assessment of hippocampal volumes on MR imaging. J Alzheimers Dis 2016;49:723-732. doi:10.3233/JAD-150559

31 Struyfs H, Sima DM, Wittens M, et al. Automated MRI volumetry as a diagnostic tool for Alzheimer's disease: validation of icobrain dm. Neuroimage Clin 2020;26:102243. doi:10.1016/j.nicl.2020.102243

32 de Boer R, Vrooman HA, Ikram MA, et al. Accuracy and reproducibility study of automatic MRI brain tissue segmentation methods. Neuroimage 2010;51(3):1047-1056. doi:10.1016/j.neuroimage.2010.03.012

33 Schippling S, Ostwaldt A-C, Suppa P, et al. Global and regional annual brain volume loss rates in physiological aging. J Neurol 2017;264(3):520-528. doi:10.1007/s00415-016-8374-y

34 FDA clears AI-based MRI interpretation assistants from Siemens Healthineers. Posted August 19, 2020. Accessed April 13, 2022. siemens-healthineers.com/en-us/press-room/press-releases/fdaclearsairadcompanionbrainmr.html

35 Dale AM, Fischl B, Sereno MI. Cortical surface-based analysis. I. Segmentation and surface reconstruction. Neuroimage 1999;9(2):179-194. doi:10.1006/nimg.1998.0395

36 Ashburner J, Friston KJ. Voxel-based morphometry – the methods. Neuroimage 2000; 11(6 pt 1):805-821. doi:10.1006/nimg.2000.0582

37 Manjón JV, Coupé P. volBrain: an online MRI brain volumetry system. Front Neuroinform 2016;10:30. doi:10.3389/fninf.2016.00030

38 Mori S, Wu D, Ceritoglu C, et al. MRICloud: delivering high-throughput MRI neuroinformatics as cloud-based software as a service. Comput Sci Eng 2016;18(5):21-35. doi:10.1109/MCSE.2016.93

39 Henschel L, Conjeti S, Estrada S, et al. FastSurfer - a fast and accurate deep learning based neuroimaging pipeline. Neuroimage 2020;219: 117012. doi:10.1016/j.neuroimage.2020.117012

40 Jenkinson M, Beckmann CF, Behrens TEJ, et al. FSL. Neuroimage 2012;62(2):782-790. doi:10.1016/j.neuroimage.2011.09.015

41 Practical Neurology. Quantitative structural MRI for neurocognitive disorders. Accessed April 13, 2022. practicalneurology.com/articles/2020-nov-dec/quantitative-structural-mri-for-neurocognitive-disorders/pdf

42 Celebrating 10 years of FDA clearance: a mid-year review from Guri Stark, CEO. CorTechs Labs 2016. Accessed April 13, 2022. cortechslabs.com/10-years-of-fda-clearance

43 Jain S, Vyvere TV, Terzopoulos V, et al. Automatic quantification of computed tomography features in acute traumatic brain injury. J Neurotrauma 2019;36(11):1794-1803. doi:10.1089/neu.2018.6183

44 Meysami S, Raji CA, Merrill DA, et al. MRI volumetric quantification in persons with a history of traumatic brain injury and cognitive impairment. J Alzheimers Dis 2019;72(1):293-300. doi:10.3233/JAD-190708

45 Mettenburg JM, Branstetter BF, Wiley CA, et al. Improved detection of subtle mesial temporal sclerosis: validation of a commercially available software for automated segmentation of hippocampal volume. AJNR Am J Neuroradiol 2019;40(3):440-445. doi:10.3174/ajnr.A5966

46 Morris JC. Clinical dementia rating: a reliable and valid diagnostic and staging measure for dementia of the Alzheimer type. Int Psychogeriatr 1997;9(suppl 1):177-178. doi:10.1017/s1041610297004870

47 den Heijer T, Geerlings MJ, Hoebeek FE, et al. Use of hippocampal and amygdalar volumes on magnetic resonance imaging to predict dementia in cognitively intact elderly people. Arch Gen Psychiatry 2006;63(1):57-62. doi:10.1001/archpsyc.63.1.57

48 Ross DE, Ochs AL, Seabaugh JM, et al. Man versus machine: comparison of radiologists' interpretations and NeuroQuant® volumetric analyses of brain MRIs in patients with traumatic brain injury. J Neuropsychiatry Clin Neurosci 2013; 25(1):32-39. doi:10.1176/appi.neuropsych.11120377

49 Ross DE, Ochs AL, DeSmit ME, et al. Man versus machine part 2: comparison of radiologists' interpretations and NeuroQuant measures of brain asymmetry and progressive atrophy in patients with traumatic brain injury. J Neuropsychiatry Clin Neurosci 2015;27(2): 147-152. doi:10.1176/appi.neuropsych.13040088

50 Bigler ED, Blatter DD, Anderson CV, et al. Hippocampal volume in normal aging and traumatic brain injury. AJNR Am J Neuroradiol 1997;18(1):11-23.

51 Nelson PT, Smith CD, Abner EL, et al. Hippocampal sclerosis of aging, a prevalent and high-morbidity brain disease. Acta Neuropathol 2013;126(2):161-177. doi:10.1007/s00401-013-1154-1

52 Lundeen TF, Seibyl JP, Covington MF, et al. Signs and artifacts in amyloid PET. RadioGraphics 2018; 38(7):2123-2133. doi:10.1148/rg.2018180160

53 Murphy EA, Holland D, Donohue M, et al. Six-month atrophy in MTL structures is associated with subsequent memory decline in elderly controls. Neuroimage 2010;53(4):1310-1317. doi:10.1016/j.neuroimage.2010.07.016

54 Barnes J, Bartlett JW, van de Pol LA, et al. A meta-analysis of hippocampal atrophy rates in Alzheimer's disease. Neurobiol Aging 2009;30(11): 1711-1723. doi:10.1016/j.neurobiolaging.2008.01.010

55 Jack CR, Bennett DA, Blennow K, et al. NIA-AA research framework: toward a biological definition of Alzheimer's disease. Alzheimers Dement 2018;14(4):535-562. doi:10.1016/j.jalz.2018.02.018

56 Gordon BA, Friedrichsen K, Brier M, et al. The relationship between cerebrospinal fluid markers of Alzheimer pathology and positron emission tomography tau imaging. Brain 2016; 139(pt 8):2249-2260. doi:10.1093/brain/aww139

57 Gordon BA, Blazey TM, Christensen J, et al. Tau PET in autosomal dominant Alzheimer's disease: relationship with cognition, dementia and other biomarkers. Brain 2019;142(4):1063-1076. doi:10.1093/brain/awz019

58 Vogel JW, Young AL, Oxtoby NP, et al. Four distinct trajectories of tau deposition identified in Alzheimer's disease. Nat Med 2021;27(5): 871-881. doi:10.1038/s41591-021-01309-6

59 Leuzy A, Chiotis K, Lemoine L, et al. Tau PET imaging in neurodegenerative tauopathies–still a challenge. Mol Psychiatry 2019;24(8):1112-1134. doi:10.1038/s41380-018-0342-8

60 Silverman DH, Small GW, Chang CY, et al. Positron emission tomography in evaluation of dementia: regional brain metabolism and long-term outcome. JAMA 2001;286(17): 2120-2127. doi:10.1001/jama.286.17.2120

61 Yeo JM, Waddell B, Khan Z, Pal S. A systematic review and meta-analysis of $^{18}$ F-labeled amyloid imaging in Alzheimer's disease. Alzheimers Dement (Amst) 2015;1(1):5-13. doi:10.1016/j.dadm.2014.11.004

62 Suppiah S, Didier M-A, Vinjamuri S. The who, when, why, and how of PET amyloid imaging in management of Alzheimer's disease–review of literature and interesting images. Diagnostics (Basel) 2019;9(2):65. doi:10.3390/diagnostics9020065

63 Haller S, Montandon M-L, Lilja J, et al. PET amyloid in normal aging: direct comparison of visual and automatic processing methods. Sci Rep 2020;10(1):16665. doi:10.1038/s41598-020-73673-1

64 Cattell L, Platsch G, Pfeiffer R, et al. Classification of amyloid status using machine learning with histograms of oriented 3D gradients. NeuroImage Clin 2016;12:990-1003. doi:10.1016/j.nicl.2016.05.004

65 Rabinovici GD, Gatsonis C, Apgar C, et al. Association of amyloid positron emission tomography with subsequent change in clinical management among Medicare beneficiaries with mild cognitive impairment or dementia. JAMA 2019;321(13):1286-1294. doi:10.1001/jama.2019.2000

66 Foster NL, Heidebrink JL, Clark CM, et al. FDG-PET improves accuracy in distinguishing frontotemporal dementia and Alzheimer's disease. Brain 2007;130(pt 10):2616-2635. doi:10.1093/brain/awm177

67 Brown RKJ, Bohnen NI, Wong KK, et al. Brain PET in suspected dementia: patterns of altered FDG metabolism. RadioGraphics 2014;34(3):684-701. doi:10.1148/rg.343135065

68 Képes Z, Aranyi Cs, Forgács A, et al. Glucose-level dependent brain hypometabolism in type 2 diabetes mellitus and obesity. Eur J Hybrid Imaging 2021;5(1):3. doi:10.1186/s41824-021-00097-z

69 Kirmess KM, Meyer MR, Holubasch MS, et al. The PrecivityAD™ test: accurate and reliable LC-MS/MS assays for quantifying plasma amyloid beta 40 and 42 and apolipoprotein E proteotype for the assessment of brain amyloidosis. Clin Chim Acta 2021;519:267-275. doi:10.1016/j.cca.2021.05.011

70 Cullen NC, Leuzy A, Janelidze S, et al. Plasma biomarkers of Alzheimer's disease improve prediction of cognitive decline in cognitively unimpaired elderly populations. Nat Commun 2021;12(1):3555. doi:10.1038/s41467-021-23746-0

71 Schindler SE, Bollinger JG, Ovod V, et al. High-precision plasma β-amyloid 42/40 predicts current and future brain amyloidosis. Neurology 2019;93(17):e1647-e1659. doi:10.1212/WNL.0000000000008081

72 Fazekas F, Chawluk J, Alavi A, et al. MR signal abnormalities at 1.5 T in Alzheimer's dementia and normal aging. AJR Am J Roentgenol 1987; 149(2):351-356. doi:10.2214/ajr.149.2.351

73 Longstreth WT, Manolio TA, Arnold A, et al. Clinical correlates of white matter findings on cranial magnetic resonance imaging of 3301 elderly people. The Cardiovascular Health Study. Stroke 1996;27(8):1274-1282. doi:10.1161/01.str.27.8.1274

74 Raji CA, Lopez OL, Kuller LH, et al. White matter lesions and brain gray matter volume in cognitively normal elders. Neurobiol Aging 2012; 33(4):834.e7-834.e16. doi:10.1016/j.neurobiolaging.2011.08.010

75 Shim YS, Yang D-W, Roe CM, et al. Pathological correlates of white matter hyperintensities on magnetic resonance imaging. Dement Geriatr Cogn Disord 2015;39(1-2):92-104. doi:10.1159/000366411

76 Greenberg SM, Vernooij MW, Cordonnier C, et al. Cerebral microbleeds: a guide to detection and interpretation. Lancet Neurol 2009;8(2):165-174. doi:10.1016/S1474-4422(09)70013-4

77 Lee J, Sohn EH, Oh E, Lee AY. Characteristics of cerebral microbleeds. Dement Neurocognitive Disord 2018;17(3):73-82. doi:10.12779/dnd.2018.17.3.73

78 Charidimou A, Boulouis G, Greenberg SM, Viswanathan A. Cortical superficial siderosis and bleeding risk in cerebral amyloid angiopathy: a meta-analysis. Neurology 2019;93(24):e2192-e2202. doi:10.1212/WNL.0000000000008590

79 Chen Y, Li Y, Lu J, Li W, Wang J. Correlation between the reduction in lenticulostriate arteries caused by hypertension and changes in brain metabolism detected with MRI. AJR Am J Roentgenol 2016;206(2):395-400. doi:10.2214/AJR.15.14514

80 Liu J, Kou Z, Tian Y. Diffuse axonal injury after traumatic cerebral microbleeds: an evaluation of imaging techniques. Neural Regen Res 2014;9(12):1222-1230. doi:10.4103/1673-5374.135330.

81 Raji CA, Henderson TA. PET and single-photon emission computed tomography in brain concussion. Neuroimaging Clin N Am 2018;28(1):67-82. doi:10.1016/j.nic.2017.09.003

82 Banerjee G, Carare R, Cordonnier C, et al. The increasing impact of cerebral amyloid angiopathy: essential new insights for clinical practice. J Neurol Neurosurg Psychiatry 2017;88(11):982-994. doi:10.1136/jnnp-2016-314697

83 VandeVrede L, Gibbs DM, Koestler M, et al. Symptomatic amyloid-related imaging abnormalities in an APOE ε4/ε4 patient treated with aducanumab. Alzheimers Dement 2020;12;12(1):e12101. doi:10.1002/dad2.12101

84 Cummings J, Aisen P, Apostolova LG, et al. Aducanumab: appropriate use recommendations. J Prev Alz Dis 2021;8(4):398-410. doi:10.14283/jpad.2021.41

85 Centers for Medicare & Medicaid Services. CMS proposes Medicare coverage policy for monoclonal antibodies directed against amyloid for the treatment of Alzheimer's disease. Published January 11, 2022. Accessed April 13, 2022. cms.gov/newsroom/press-releases/cms-proposes-medicare-coverage-policy-monoclonal-antibodies-directed-against-amyloid-treatment

86 ADUHELM (aducanumab-avwa) injection, for intravenous use. Initial US approval: 2021. Revised June 2021. Accessed April 13, 2022. www.accessdata.fda.gov/drugsatfda_docs/label/2021/761178s000lbl.pdf

87 Kim WS, Kågedal K, Halliday GM. Alpha-synuclein biology in Lewy body diseases. Alz Res Ther 2014;6(5):73. doi:10.1186/s13195-014-0073-2

88 McKeith IG, Boeve BF, Dickson DW, et al. Diagnosis and management of dementia with Lewy bodies: fourth consensus report of the DLB Consortium. Neurology 2017;89(1):88-100. doi:10.1212/WNL.0000000000004058

89 Surendranathan A, O'Brien JT. Clinical imaging in dementia with Lewy bodies. Evid Based Ment Health 2018;21(2):61-65. doi:10.1136/eb-2017-102848

90 Kanzaki T, Higuchi T, Takahashi Y, et al. Improvement of diagnostic accuracy of Parkinson's disease on I-123-ioflupane single photon emission computed tomography ($^{123}$I FP-CIT SPECT) using new Japanese normal database. Asia Ocean J Nucl Med Biol 2020;8(2):95-101. doi:10.22038/AOJNMB.2019.43685.1290

91 Antonini A, Benti R, De Notaris R, et al. 123I-Ioflupane/SPECT binding to striatal dopamine transporter (DAT) uptake in patients with Parkinson's disease, multiple system atrophy, and progressive supranuclear palsy. Neurol Sci 2003;24(3):149-150. doi:10.1007/s10072-003-0103-5

92 Ogawa T, Fujii S, Kuya K, et al. Role of neuroimaging on differentiation of Parkinson's disease and its related diseases. Yonago Acta Med 2018;61(3):145-155. doi:10.33160/yam.2018.09.001

93 Bega D, Kuo PH, Chalkidou A, et al. Clinical utility of DaTscan in patients with suspected Parkinsonian syndrome: a systematic review and meta-analysis. NPJ Parkinsons Dis 2021;7(1):43. doi:10.1038/s41531-021-00185-8

94 Ishii K, Kanda T, Harada A, et al. Clinical impact of the callosal angle in the diagnosis of idiopathic normal pressure hydrocephalus. Eur Radiol 2008;18(11):2678-2683. doi:10.1007/s00330-008-1044-4

95 Wu EM, Ahmadieh TY, Kafka B, et al. Ventriculoperitoneal shunt outcomes of normal pressure hydrocephalus: a case series of 116 patients. Cureus 2019;11(3):e4170. doi:10.7759/cureus.4170

96 Halperin JJ, Pascual-Leone A, Saper CB. Symptomatic hydrocephalus with normal cerebrospinal pressure and Alzheimer's disease. Ann Neurol 2020;88(4):685-687. doi:10.1002/ana.2587

## DISCLOSURE

*Continued from page 800*

as a consultant for Siemens and Eisai Co, Ltd that are relevant to American Academy of Neurology interests or activities. The blood-based amyloid test is licensed by C2N and was cofounded by colleagues of Dr Benzinger. Washington University will receive royalties from this test, but Dr Benzinger will not receive personal compensation from it.